Iraqi Journal of Science, 2026, Vol. 67, No. 4, pp: 2484- 2501
DOI: 10.24996/ijs.2026.67.4.45

ISSN: 0067-2904

Analysis of Wind Speed Characteristics and Wind Turbine Parameters Estimation Corresponding to North Part of Iraq

Firas A. Hadi[1*], Rafa Abbas Hassan Al-Baldawi[1], Hussein T. Salloom[2], Ethar Yahya Salih[1]

College of Energy and Environmental Sciences, Al-Karkh University of Science, 10081, Baghdad, Iraq
[2]Al-Nahrain Renewable Energy Research Center, Al-Nahrain University, Baghdad, Iraq

Received: 29 /9/2024 Accepted: 12/4/2025 Published: 30/4/2026

Abstract

Wind energy is considered the world's second sustainable energy source after solar energy was utilized to generate electrical energy. Iraq's accession to the Paris Climate Agreement encouraged the government to involve small and large projects in generating electricity from renewable energy sources, including wind. This requires preliminary studies on the feasibility of investing in renewable energy sources in Iraq. This work was concerned with analyzing wind energy for the city of Sinjar-Nineveh in northern Iraq to determine the extent of the potential of wind energy in generating electrical energy in that region. The wind speed and direction in the area were analyzed at three altitudes for 44 years. The results showed that the northwest direction is dominant, and the average speed is 4.6, 4.8, and 5.0 m/s at altitudes of 50, 70, and 100 m, respectively. Among the Maximum Likelihood, Least Squares, and WAsP methods, the Least Squares method was the best in estimating the Weibull coefficients. The results showed that the power density equals 116, 130, and 146 W/m2 at the above altitudes. Four types of turbines were assumed to achieve the highest capacity factor within the study area using Windographer program analysis. It was concluded that the specifications of the EWT DW52-500 turbine (WT-A) achieved the highest energy production rates at the three altitudes in the study area with a capacity factor of 19% before mechanical and electrical losses and 15% after assuming these losses.

Keywords: Gases emission; Renewable energy; Sustainable energy; Wind energy.

للجزء تحليل خصائص سرعة الرياح وتقدير معلمات توربينات الرياح الموافقة الشمالي من العراق

فراس عبد الرزاق عبد الهادي[1]*، رافع عباس حسن البلداوي[1]، حسين ثامر سلوم[2]، ايثار يحيى صالح[1]

[1] كلية علوم الطاقة والبيئة، جامعة الكرخ للعلوم، بغداد، العراق

[2] مركز بحوث الطاقة المتجددة، جامعة النهرين، بغداد، العراق

الخلاصة

*Email: Firas.a.hadi@kus.edu.iq

يعاني العراق منذ فترة طويلة من نقص الطاقة الكهربائية، ومن ناحية أخرى فإن مصادر الطاقة البديلة مثل الطاقة المتجددة المتمثلة بالطاقة الشمسية وطاقة الرياح والكتلة الحيوية لم يتم استغلالها بشكل كاف لحد الان، بالرغم من انها قد تكون حلاً لنقص الطاقة وأزمة الوقود في البلاد في الوقت الحاضر وفي المستقبل. كما أن مصادر الطاقة المتجددة لها بعد مهم آخر في الحفاظ على البيئة وتقليل انبعاث الغازات المسببة للاحتباس الحراري. يختلف توافر هذه المصادر من مكان إلى آخر كما إن سهولة استخدامها تعتمد على أماكن توافرها. وتعد طاقة الرياح هي ثاني مصدر للطاقة المستدامة في العالم، بعد الطاقة الشمسية، والتي يتم استغلالها لتوليد الطاقة الكهربائية. بالإضافة إلى ذلك، شجع انضمام العراق إلى اتفاقية باريس للمناخ الحكومة على إشراك المشاريع الصغيرة والكبيرة في توليد الكهرباء من مصادر الطاقة المتجددة بما في ذلك الرياح. وهذا يتطلب دراسات أولية حول جدوى استثمار مصادر الطاقة المتجددة في العراق. يتعلق هذا العمل بتحليل طاقة الرياح لمدينة سنجار – نينوى في شمال العراق لتحديد مدى إمكانية طاقة الرياح في توليد الطاقة الكهربائية في تلك المنطقة. حيث تم تحليل سرع الرياح واتجاهها في تلك المنطقة على ثلاث ارتفاعات ولمدة 44 سنة. أظهرت النتائج ان الاتجاه الشمالي الغربي هو السائد وان معدل السرع هو 4.6 ، 4.8، و 5.0 م/ثا على الارتفاعات 50، 70، 100م على التوالي. ومن بين الطرق Maximum likelihood، Least squares، و WAsP تبين ان الطريقة Least squares هي الأفضل في تقدير معاملات ويبل. النتائج بينت ان كثافة القدرة تساوي 116، 130، و146 واط/م2 على الارتفاعات السابقة. كما افترض وجود أربعة أنواع من التوربينات وبما يحقق اعلى عامل للسعة مع منطقة الدراسة باستخدام تحليلات برنامج Windographer. كما تم الاستنتاج ان مواصفات التوربين EWT DW52−500 والمكنى بالبحث (WT−A) في هذه الدراسة قد حققت اعلى نسب إنتاجية للطاقة وعلى الارتفاعات الثلاثة في منطقة الدراسة وبنسبة عامل سعة 19% قبل الخسائر الميكانيكية والكهربائية و15% بعد افتراض هذه الخسائر

.1. Introduction

Daily power interruption is a major issue among Iraqi households because of a shortage of electricity generation considering overloaded electricity grids and old power plants. The electrical interruption could reach up to 20 hrs. in Iraq daily, forcing residents to rely mainly on “household generators” and “neighborhood generators.” As a result, higher CO_2 emissions are attained from the stated electricity generation methods due to diesel engine usage [1]. Wind energy is one of the most thriving and growing renewable energy sources. The installed capacity of wind power is estimated to be 906 GW in 2022, which can be used to generate electricity in some isolated and remote places.

Meanwhile, in Iraq, renewable sources are almost limited to solar, wind, and hydropower [2, 3]. The demand for energy in Iraq is constantly increasing [4]. An increase of 4.7%, within the period from 2008 to 2020, was recorded as 4,000 MW, equivalent to 300 MW annually. The demand for primary energy increased by 5.5% in 2020, reaching 15 million tons of oil equivalent, exceeding 7.5 million tons in 2008. Wind-based energy is the least expensive among the different types of renewable energy [5]. Several research groups have recently dedicated themselves to investigating and predicting wind energy in Iraq [4, 6, 7].

Iraq does not suffer exceptionally high yearly wind speeds because of its geographic location. Studies conducted in Iraq on wind energy typically show that wind speeds vary from 5 to 10 m/s [6]. In Iraq, wind energy is separated into three areas: 48% of these areas have low annual wind speed, 35% is between 3.1 to 4.9 m/s, and 8% is high, and the remaining values are calm [7, 8]. It has been noted that summer winds have higher speeds than winter winds, which is very positive because they will meet the increasing demand in the summer for electrical energy due to ventilation and cooling purposes compared to the winter months. Iraq is not a cost-effective location for wind turbine construction compared to other countries since wind turbine performance and wind speed depend on the available wind speed, which must fulfill the needs of the turbines installed there. For low wind speeds, a complex design needs to be created [9]. Since wind speeds vary from one location to another for many reasons,

including surface roughness, topography, and weather conditions, wind energy requires studying different locations in the country to benefit from any promising part. Sinjar-Nineveh is one of the locations in Iraq chosen for study in this research to determine the extent of the site's promise for wind energy production [10].

2. Materials and Methods

It is possible to get an idea of the site's wind speed, distribution, and ground surface roughness using Global Wind Atlas maps (GWA3), which helps us know how wind energy can be utilized. The study site is in Iraq around Mount Sinjar, Figure 1 (a). It is located near the Syrian border between Ninewa Iraqi Governorate and Al-Hasakah Syrian Governorate, near the city of Sinjar, and about 416,000 km away from the capital of Iraq (Baghdad). Windographer software was used for statistical analysis and visualization of wind resource data. This software lets data quickly be imported from various formats or the NASA website [11].

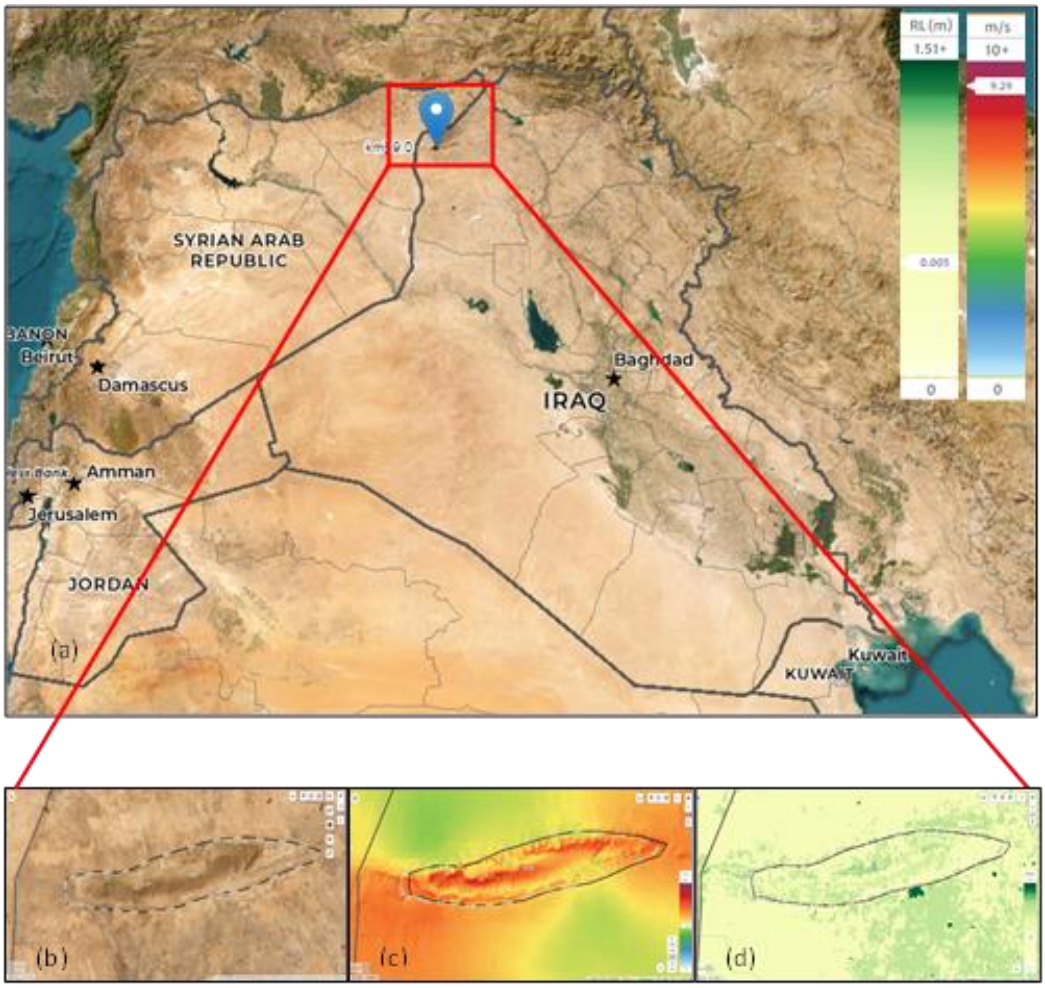

Figure 1: Features of Sinjar site [8] (a) Sinjar location in Iraq (b) Annual mean wind speed at 100m altitude (d) The surface roughness length at Sinjar location

Figure 1(a and b) shows a satellite image, which gives an idea of the area's topography. The wind speed on Mount Sinjar has high values, reaching about 9m/s at 100m height from the earth's surface. Figure 1(c) represents the wind of this region, which lies between gale and strong gale according to Beaufort's wind scale description [12]. Figure 1(d) represents the surface roughness length of the ground, which is located between 0.005-0.3m; this shows that

the site's roughness scale is relatively low, and the region can be described in terms of the roughness length lies between “Snow surface” and “Many trees, few buildings,” [13]. The following subsections will describe the data, analytical techniques, and tools utilized in the project.

3. Data Acquisition

The analysis was conducted using data on duration 42 years mean wind speed observed at a height 50 m above the ground starting from 1-1-1980 through 1-11-2023 using 10-minute time steps. The Windowgrapher software allows data to be downloaded from the NASA website [14]. The information was gathered from the Sinjar district on the NASA website at Latitude 36.500° and Longitude 41.875°, Table 1.

Table 1: Location statistics.

Sinjar	
Latitude	36.500 deg
Longitude	41.875 deg
Elevation	50 m, 70 m, 100 m
POR Start	1-1-1980
POR End	1-11-2023
Duration	44 years
Time step	10 minutes
Mean wind speed at 50 m	4.8 m/s
Power density at 50 m	110 W/m^2

4. Methodology

The wind is affected by multiple aspects, like temperature, pressure, surface shape, and obstacles. It changes from one season to another, during one day, and from one region to another. Therefore, statistical methods are relied upon to study wind energy. Figure 2 shows the path followed in the research methodology to evaluate wind resources, the appropriate turbine type, and the resulting energy.

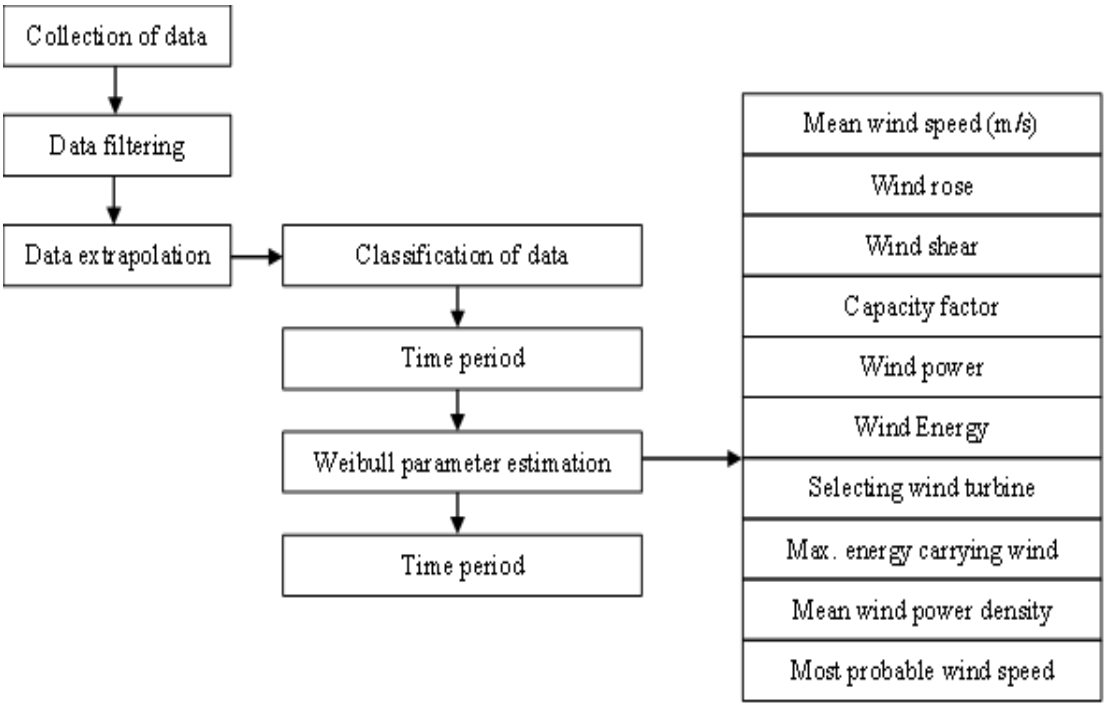

Figure 2: Research method used to evaluate wind resources and energy output.

4.1 Mathematical Basis

An expression for the wind shear could be expressed as [15]:

$$\alpha = \ln(v_2) - \ln(v_1)/\ln(z_2) - \ln(z_1) \quad (1)$$

herein, wind speed is represented by v_1 and v_2 at z_1 and z_2 heights, respectively; α represents the wind shear exponent, which can be given by [16]:

$$\alpha = \frac{0.37 - 0.088 \ln(v_{ref})}{1 - 0.088 \times \ln(\frac{z_{ref}}{10})} \quad (2)$$

where, v_{ref} represents reference wind velocity at hub height z_{ref} [17].

4.2 Weibull Probability Distribution Function

This can be utilized if wind energy is advantageous in a certain location, as given by [18].

$$f(v) = \left(\frac{k}{A}\right)\left(\frac{v}{A}\right)^{k-1} exp\left[-\left(\frac{v}{A}\right)^{k}\right], k > 0, v > 0, A > 1 \quad (3)$$

Where both k and A- are Weibull parameters, they are the so-called scale factor (A m/s) and Shape factor (k), respectively.

4.3 Mean Wind Speed

The mean wind speed v_{avg} is represented by [19].

$$v_{avg} = \left(\frac{1}{n}\sum_{i=1}^{n} v_i^3\right)^{1/3} \quad (4)$$

While variance and standard deviation are represented by [20].

$$\sigma^2 = \frac{1}{n-1}\sum_{i=1}^{n}\left(v_i - v_{avg}\right)^2 \quad (5)$$

$$\sigma = \sqrt{\frac{1}{n-1}\sum_{i=1}^{n}\left(v_i - v_{avg}\right)^2} \quad (6)$$

4.4 Weibull Parameters

For any potential location where the conversion of wind energy equipment is to be installed, precisely estimating the Weibull parameters is essential. Below, three methods were utilized in this work to estimate Weibull parameters:

4.4.1 Maximum Likelihood Method

A measured wind speed distribution is fitted to a Weibull distribution utilizing the maximum likelihood method (MLM). This method involves iteratively obtaining the Weibull k parameter using the following equation [21, 22].

$$k = \left(\frac{\sum_{i=1}^{n} v_i^k \, ln(v_i)}{\sum_{i=1}^{n} v_i^k} - \frac{\sum_{i=1}^{n} ln(v_i)}{n}\right)^{-1} \quad (7)$$

$$A = \left(\frac{\sum_{i=1}^{n} v_i^k}{n}\right)^{1/k} \quad (8)$$

4.4.2 Least Square Method

The cumulative density function (CDF) of Weibull distribution can be presented as [23]:

$$F(v) = 1 - e^{-\left(\frac{v}{A}\right)^k} \quad (9)$$

Rearranging Eq. (9) and taking logarithms for both sides,

$$ln\left[-ln\left(1 - F(v_i)\right)\right] = k \ ln\, v_i - k \ ln\, A \quad (10)$$

Which represents a straight-line equation such that:

$$y_i = a_i + b \quad (11)$$

$$y_i = ln\left[-ln\left(1 - F(v_i)\right)\right];\ a = k;\ x_i = ln\, v_i\ ;\ b = -k\ ln\, A \quad (12)$$

By comparing Eq. 10 with Eq. 11,

Thus, Weibull parameters can be written as:

$$k = \frac{n\sum_{i=1}^{n} x_i y_i - \sum_{i=1}^{n} x_i \sum_{i=1}^{n} y_i}{n\sum_{i=1}^{n} x_i^2 - \left(\sum_{i=1}^{n} x_i\right)^2} \quad b = -k\ ln\, A$$

$$(13) A = exp\left(\frac{k\sum_{i=1}^{n} x_i - \sum_1^n y_i}{nk}\right) \quad (14)$$

4.4.3 WAsP

Using a function optimization approach, it is based on the distribution's energy content and finds the Weibull parameters that equal the wind speed cube and best suit wind speed distribution.

The wind speed probability greater than/equal to $v - 1$ and lower than v is [24].

$$P(v) = e^{-\left(\frac{v-1}{A}\right)^k} - e^{-\left(\frac{v}{A}\right)^k} \quad (15)$$

It may define the probability function P_v As follows:

$$P_v = P(v) + \varepsilon \quad (16)$$

The scale factor r for cube wind speed using Eq. (8) can be written as:

$$A = \left(\frac{v_m^3}{\Gamma\left(1+\frac{3}{k}\right)}\right)^{1/3} \quad (17)$$

Thus, k can be estimated by substituting Eq. (17) in Eq. (15), then the result in Eq. (16) yields,

$$\sum_{i=1}^{n}[P_{v_i} - e^{-\left(\frac{(v_i-1)\left(\Gamma\left(1+\frac{3}{k}\right)\right)^{\frac{1}{3}}}{v_m}\right)^k} + e^{-\left(\frac{v_i\left(\Gamma\left(1+\frac{3}{k}\right)\right)^{\frac{1}{3}}}{v_m}\right)^k}]^2 = \sum_{i=1}^{n}(\varepsilon)^2 \quad (18)$$

P_{v_i} = the probability of ith bin wind speed, n = b_{in} number for wind speed histogram, v_i = highest wind speed value for the i^{th} bin, v_m^3= mean cube.

After finding k, the scale factor is calculated by Eq. (17).

4.5 Wind power density calculation

Mathematically, wind power is designated as [25]:

$$W_p = \frac{1}{2}\rho A_T c_p v^3 \quad (19)$$

Where, c_p is Betz limit (40-50 % for large turbines, 20-30 % for smaller turbines); A_T is wind turbine rotor area; ρ is the air density. Now, wind power density from Eq. (17) is denoted by:

$$W_{pd} = \frac{W_p}{A_T} = \frac{1}{2}\rho c_p v^3 \quad (20)$$

By Weibull representation,

$$P_w = \frac{1}{2}\rho A^3 \Gamma\left(1 + \frac{3}{k}\right) \quad (21)$$

where Γ is the gamma function.

4.6 Wind Energy Assessment

It represents the quantity of energy (kWh) that can be extracted from the wind at a specific place, and it is an essential factor in assessing a site's viability for wind energy production. It was calculated by multiplying the power curve of the wind turbine and Weibull site representation as follows:

$$E = T\int_0^\infty P(v)f(v)dv \quad (22)$$

where $f(v)$ is the Weibull pdf of wind speeds (v), P is the wind turbine power curve, and T is the period [23].

$$E = T\int_0^\infty \left(\frac{k}{A}\right)\left(\frac{v}{A}\right)^{k-1} exp\left[-\left(\frac{v}{A}\right)^k\right] P(v)d(v) \quad (23)$$

4.7. Capacity Factor

The features of the wind resource and the design of the turbine affect how much electricity a wind turbine can produce. These parameters affect the capacity factor, which is the proportion of energy generated annually to energy generated by wind turbines operating at rated power in a specific time frame [25].

$$C_F = \frac{AEP}{Rated\ output \times T} \quad (24)$$

4.8 Power Coefficient

The ratio of power extracted by the turbine (P_T) to the total power contained in the wind resource (P_W) is known as the power coefficient (C_P).

$$C_P = \frac{P_T}{P_W} \quad (25)$$

4.9 Matching Between Wind Turbine and The Selected Site

The data of wind speed for the study site, which is derived from the Weibull function, and the characteristics of commercial wind turbines are compared to determine which turbine is most compatible with the site. A group of turbines is selected for study and comparison. This group will have a turbine with the highest capacity factor, which will have the highest generating capacity [7]. The normalized power curve approach may determine the best turbine to set at the location. The turbine performance index (TPI) curve derived from the normalized curves was used to determine the ideal speed parameters, v_C, v_r, and v_f, for site matching to produce more energy at higher C_f [12].

5. Results and Discussion

Data was measured at 50 m altitude and synthesized at 70 m and 100 m. The following sections discuss the results of evaluating wind energy resources, their characteristics, predicted energy output, and the identification of the best wind turbine compatible with the study site.

5.1 Site Wind Shear Assessment

Because of various physical phenomena, wind shear varies depending on the location and time of day. This parameter is helpful as it yields precise wind speed estimations at higher altitudes and accurate energy production assessment using the previous altitude data. The hourly wind speed means readings at 50, 70, and 100 m are utilized to calculate the values of wind shear exponent, accounting for the entire data set. The mean coefficient of wind shear at

the location is 0.11286 (Figure 3). The highest value of 0.11293 was recorded in June, while the lowest value of 0.11280 was recorded in December. The value of the coefficient is affected by temperature such that at high temperatures (summer), the air becomes turbulent, and thus higher values of wind shear are perceived, and its opposite was observed at lower temperatures; this is why wind shear is low in winter and high in summer at that location. Through Figure 4, it is possible to know how the mean wind shear factor changes during the hours of the day, as this figure shows the variant of the daily profile of mean speed shear as a variable with the hours of the day through all study periods (44 years). The value of the wind shear factor lies between 0.11284 and 0.11286; it can take the final value, which is 0.113.

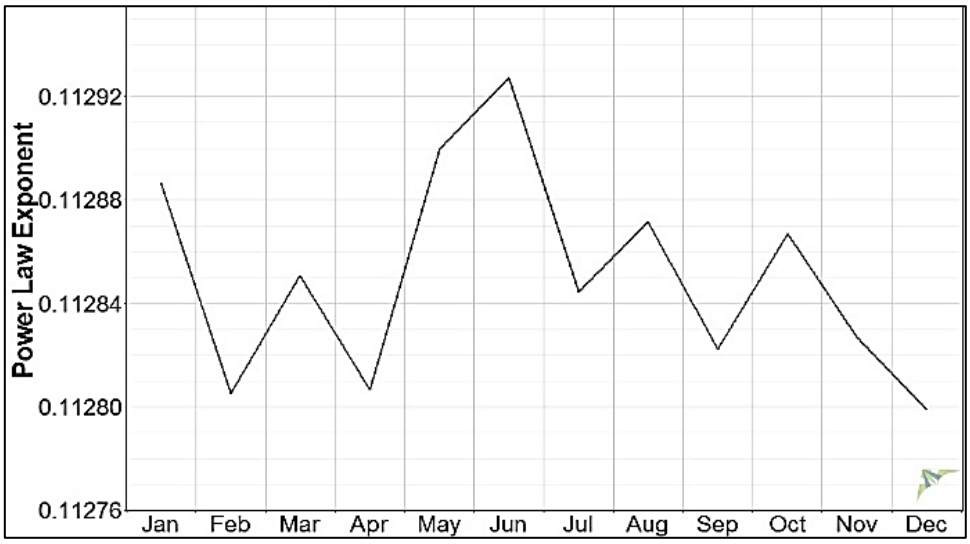

Figure 3: Wind shear coefficient of the location throughout a whole year.

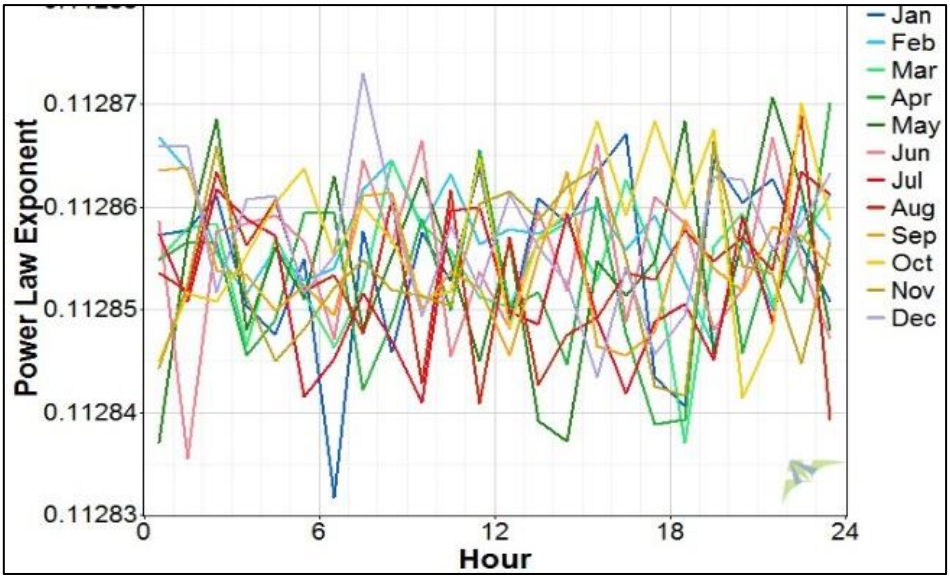

Figure 4: Daily wind shear profile.

5.2 Diurnal wind variation

The daily average wind speed (per 24 hours) at three heights, 50, 70, and 100 m, is displayed in Figure 5 from January 1, 1980, to January 5, 2022. Because of the rising temperatures when daylight approaches, wind speeds grow from six in the morning until six in the evening, when they reach their greatest value. Wind speeds decline around six o'clock, with the evenings growing colder and the daytime hours growing shorter.

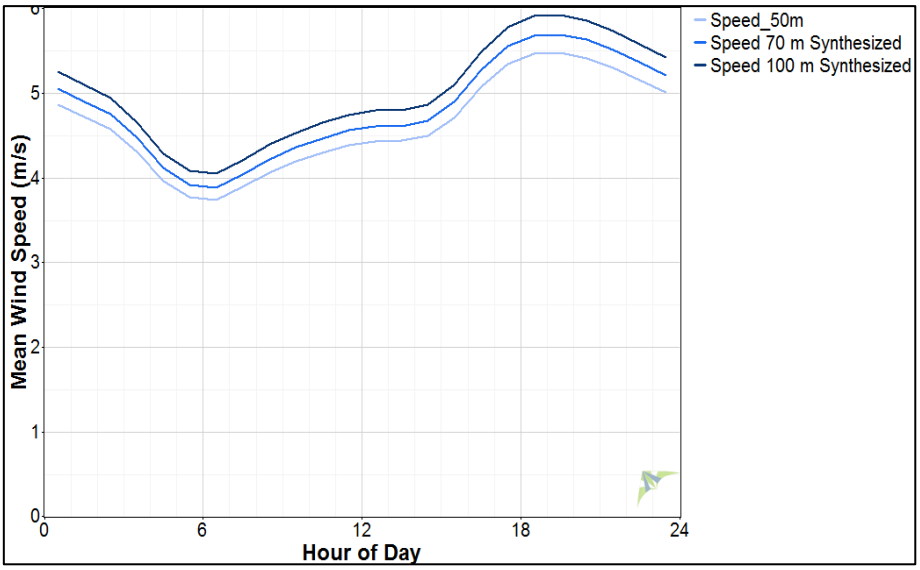

Figure 5: Mean diurnal profile.

5.3 Monthly wind variation

The monthly mean wind variance at three heights, 50, 70, and 100 m, was assessed. The wind speed measurements were highest throughout the summer and lowest during the winter. The wind variance is highest in the summer between 15:00 and 0:00 hours daily. Similarly, the lowest points of the winter season were noted at around 6:00. Figure 6 shows the monthly diurnal wind speed fluctuation. Summertime has the greatest wind speeds at all relevant measurement heights, while winters have the lowest. The most possible wind speed theory was utilized to study the wind. It indicates the value that comes up most frequently throughout gathering data. As a result, the most probable winds at 50, 70, and 100 m have the highest values in Jun and July at 8 m/s.

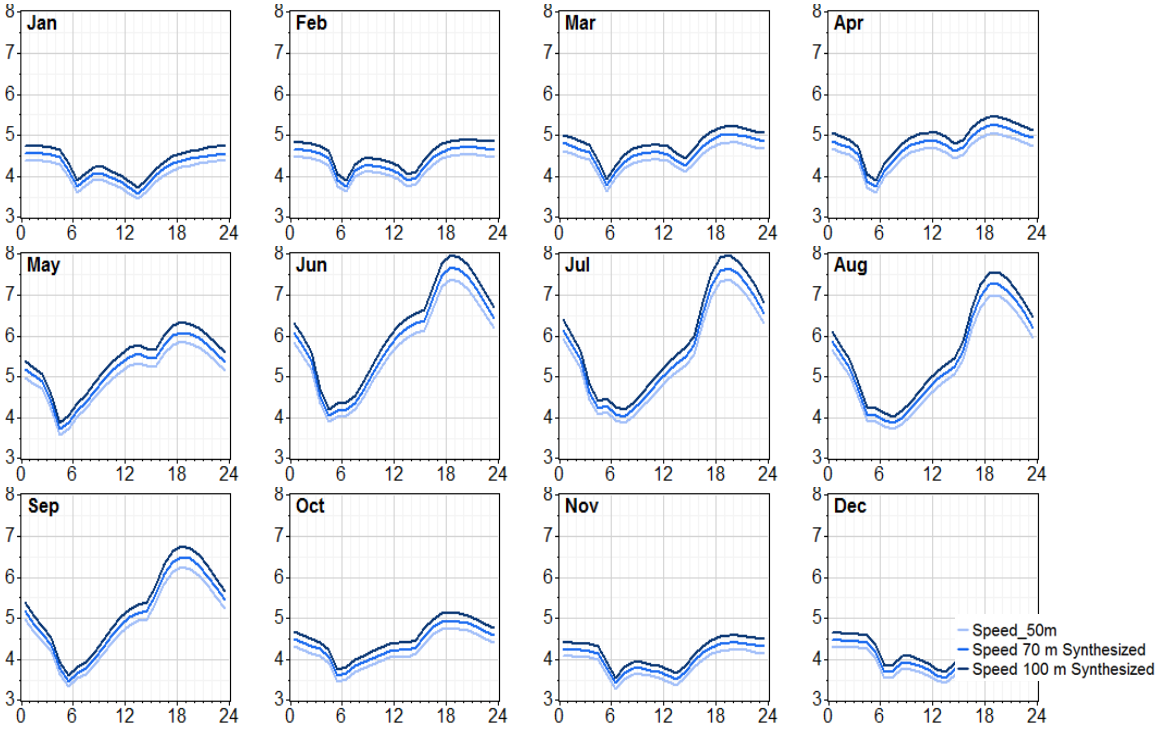

Figure 6: Mean wind speed monthly profile at 50, 70, and 100 heights.

5.4 Wind speed and direction

Figure 7 elucidates the relationship between wind direction and speed during the years of study. It is clear that there are two prevailing directions at all times of the year, the northwest and the southeast, and this applies to all altitudes of 50, 70, and 100 m. It was noted that the frequency of wind in the northwest direction exceeds the southeast. The wind speeds between 4-8 m/s blew from 270º, exceeding 6% of the time at 50 m and 70 m height, while wind speeds between 5-10 m/s at 100 m height blew from the same direction, exceeding 6% of the time. On the other hand, the wind speeds between 8-12 m/s blew from 112.5º about 4% of the time at 50 m and 70 m height, while wind speeds between 10-15 m/s at 100 m height blew from the same direction about 4% of the time.

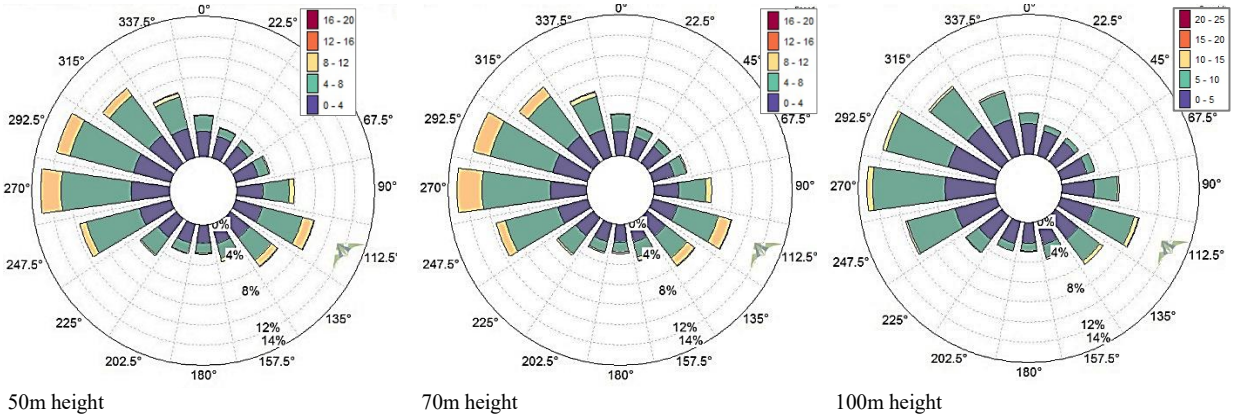

Figure 7: Frequency of wind speed vs. wind direction.

The purpose of comparing wind speeds at different heights with blowing directions (Figure 8) is to demonstrate how the wind direction changes at different heights; this matter serves greatly in the wind farm geometrical design and how these turbines are distributed at the study site.

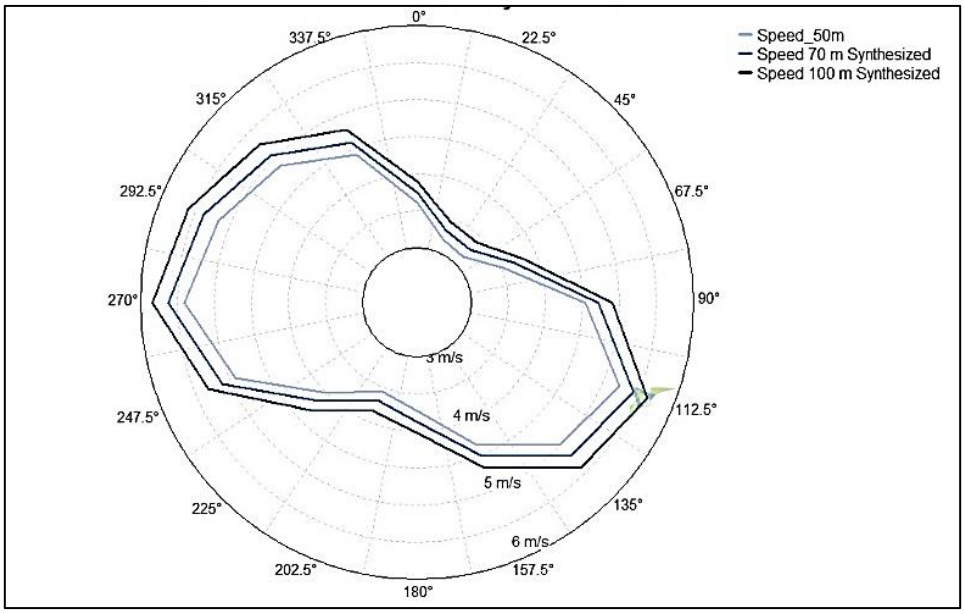

Figure 8: Frequency of wind speed vs. wind direction.

5.5 Analysis of wind speed variation

The research employed wind data gathered over 44 years beginning in 1980. 50, 70, and 100 m were the heights at which wind analysis was done. Table 2 lists the mean, maximum, minimum, and accompanying standard deviations at different proceedings heights. At 50, 70, and 100 m, the average wind speeds were determined to be 4.6, 4.8, and 5.0 m/s; Table 2. Table 2 illustrates how wind speed rises as height does.

The annual mean variation of wind speed at the three measurement heights is shown in Figure 9; the highest recorded wind speeds were 4.8, 5.0, and 5.2 m/s in 2008, while the lowest wind speeds were 4.4, 4.6, and 4.8m/s in 1996.

Table 2: Wind statistics.

Variable	Speed 100 m Synthesized	Speed 70 m Synthesized	Speed 50 m Synthesized
Measurement height (m)	100	70	50
Mean wind speed (m/s)	5.0	4.8	4.6
Min wind speed (m/s)	0.011	0.010	0.010
Max wind speed (m/s)	20.568	19.771	19.020
Std. Dev.	2.5	2.4	2.3
Mean air density (kg/m3)	1.221	1.221	1.221

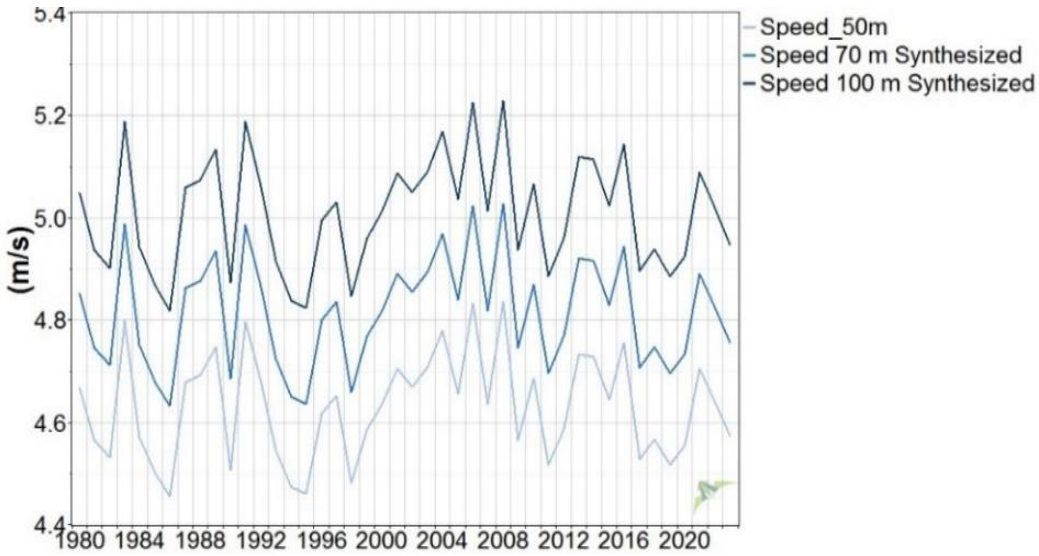

Figure 9: Annual wind speed variation.

5.6 Weibull parameters estimation methods

Weibull parameters, such as characteristics and resulting strength, are essential for investigating wind properties. The Weibull probability distribution function delivers a better fit if it is attained accurately, and the best-accurate distribution function is the one that best fits the actual data, which requires the calculation of Weibull parameters k and *A*. Three methods described previously were used to find the Weibull parameters (Maximum likelihood, Least squares, and WAsP); Figure 10.

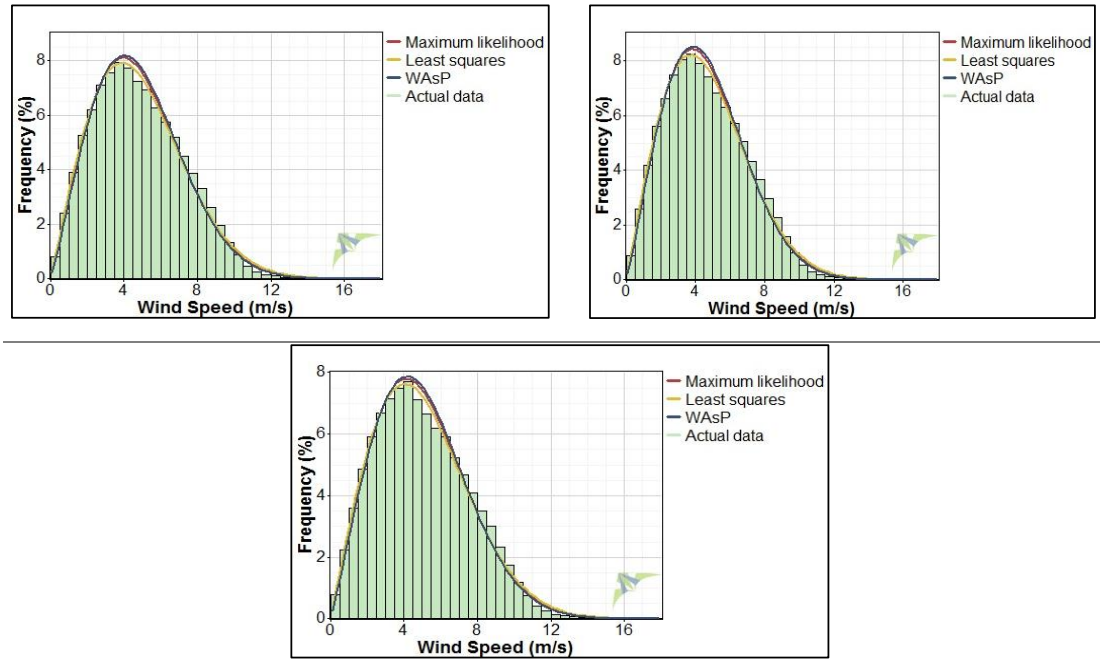

Figure 10: Pdf analysis and Weibull parameters estimation.

The value of the Coefficient of determination (R^2) at each different height. Table 3 is 0.996, which indicates that the least squares method is the closest to representing actual data. Therefore, the results of both Weibull parameters (k and A) extracted from this method at different heights will be adopted to obtain subsequent results. The values of (k and A) at 50 m, 70 m, and 100 m heights are, respectively, (2.026, 5.256), (2.026, 5.463) and (2.026, 5.674). The power density values at the three different heights fall between 100-200 W/m^2, and these values are classified within the poor class according to wind power density classes created by the National Renewable Energy Laboratory NERL [26].

Table 3: Wind speed distribution analysis.

Height	Algorithm	Weibull		Mean	Power Density	R^2
		k	A (m/s)	(m/s)	(W/m^2)	
50 m	Maximum likelihood	2.082	5.225	4.628	111.5	0.994
	Least squares	2.026	5.256	4.657	116.7	0.996
	WAsP	2.123	5.242	4.642	110.5	0.992
	Actual data	(2,305,440 time steps)		4.632	110.4	
70 m	Maximum likelihood	2.082	5.431	4.811	125.2	0.994
	Least squares	2.026	5.463	4.840	130.9	0.996
	WAsP	2.123	5.449	4.825	124.1	0.992
	Actual data	(2,305,440 time steps)		4.815	124.0	
100 m	Maximum likelihood	2.082	5.649	5.004	141.0	0.994
	Least squares	2.026	5.674	5.027	146.8	0.996
	WAsP	2.121	5.667	5.019	139.8	0.993
	Actual data	(2,305,440 time steps)		5.008	139.5	

5.7 Estimation of energy and wind power density

Table 4 shows the computed energy and wind power density values at diverse heights. The estimated wind power density ranged from 0 to 4,200 W/m^2, with an overall mean value of 116 W/m^2 at 50 m. According to estimates, the mean wind power density at 70 and 100 m are 130 and 146 W/m^2, respectively.

Similarly, the minimum values of energy density are zero at all heights, while the maximum values at 50, 70, and 100 m are 36,792, 41,329, and 46,533 kWh/m^2/y, with mean values equal to 965, 1083, and 1814, respectively.

Table 4: Annual wind power density and annual energy density.

Height (m)	Power Density (W/m^2)			Energy Density (kWh/m^2/y)		
	Max	Min	Mean	Max	Min	Mean
50	4,200	0.0	116	36,792	0.0	965
70	4,718	0.0	130	41,329	0.0	1083
100	5,312	0.0	146	46,533	0.0	1814

The monthly average values of wind energy and power densities are shown in Figures 11 and 12, respectively. Both have higher summer values and lower winter values, with June being the highest and November being the lowest. This helps produce more energy during the peak demand period in the summer, reducing the amount of fossil fuels consumed.

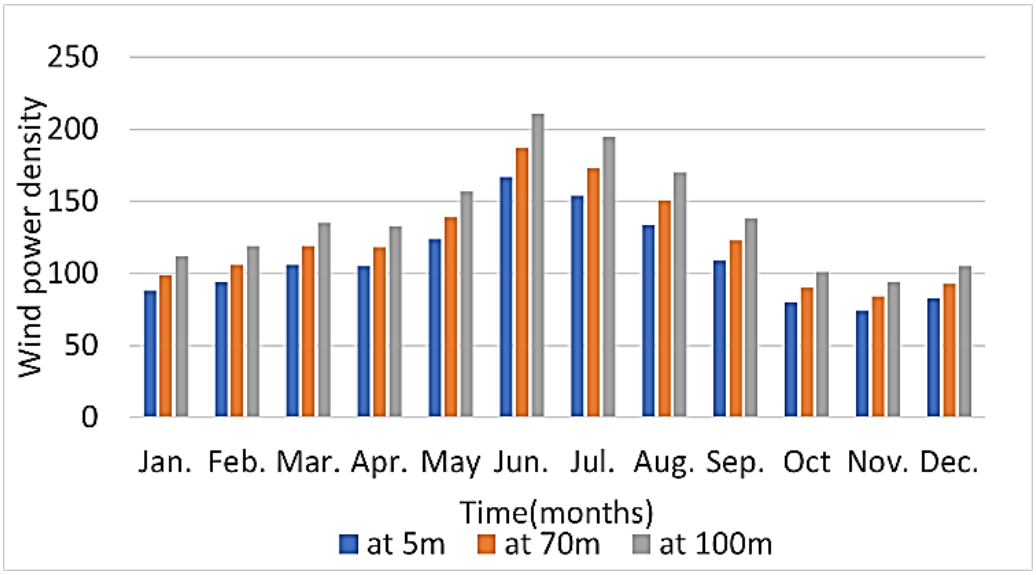

Figure 11: Wind power density (W/m2) for a year.

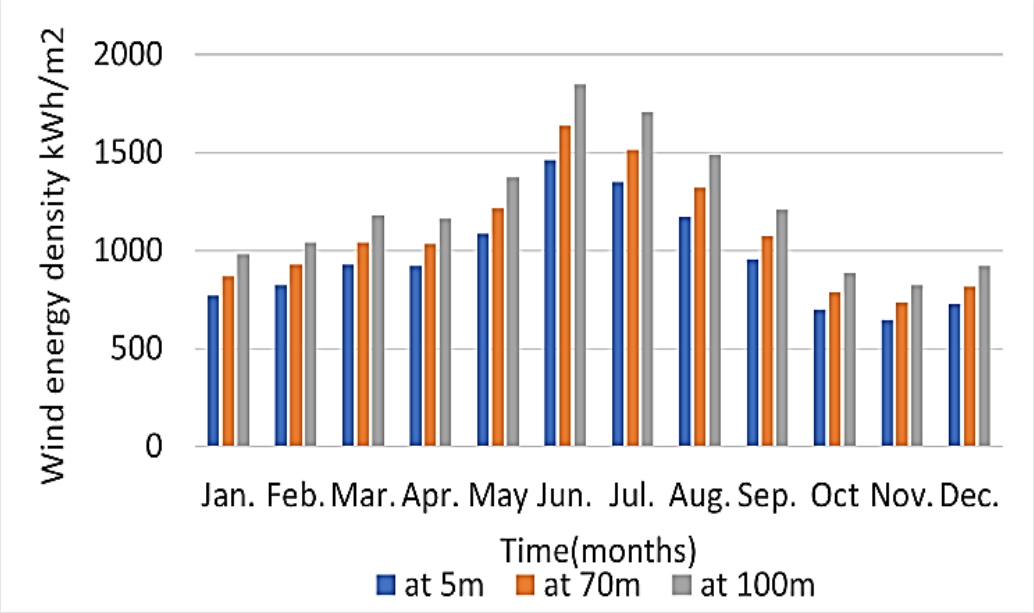

Figure 12: Energy density (kWh/m2) for a year.

5.8 Wind turbine output estimation

To know the specifications of the optimal turbine to work at the study site hypothetically, different wind turbines with different specifications and rated power are selected to estimate the annual wind power and energy production. Four wind turbines are chosen with technical specifications listed in Table 5. Figure 13 illustrates the turbines' power curves.

Table 5: Characteristics of wind turbines**.**

Wind Turbines Code	Wind Turbines	Cut-in speed (m/s)	Cut-out speed (m/s)	Rated power (kW)	Rated speed (m/s)	Rotor diameter (m)
WT-A	EWT DW52-500	3.0	25.0	500	10.0	52.0
WT-B	Enercon E33/330 kW	3.0	25.0	300	11.5	33.0
WT-C	Northern Power 100-21	3.0	25.0	100	15.0	20.7
WT-D	Legerwey FB18	3.0	25.0	80	14.0	18.0

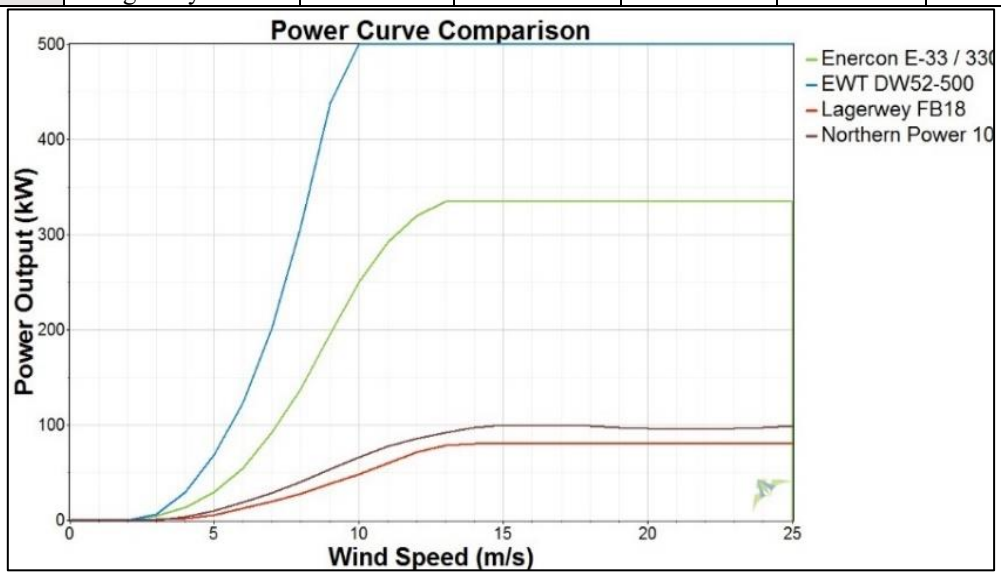

Figure 13: The wind turbine's power curve size (kW) indicated by the manufacturer.

A smaller rated speed value indicates a machine's greater performance. In this context, turbine A possesses the lowest rated speed of 10 m/s and is anticipated to perform highly compared to others. The wind turbine power curves and the frequency distribution were used to calculate the annual wind power and energy yields as well as capacity factors (CF) at different hub heights (50 m,70 m, and 100 m), taking into account the percentage of electrical and mechanical losses during the generation process (estimated by Windographer software), which is estimated at 17.7%; Table 6.

The wind turbine "WT-A" produced maximum mean power output, annual energy output, and CF after losses of 78 kW, 683,832 kWh, and 15.6% at 50 m height. At the height of 70 m, the results of maximum mean power output, annual energy output, and CF after losses of 98.2 kW, 859,842 kWh, and 19.6%, respectively, belong to turbine "WT-A." This is the case at a height of 100 m; turbine "WT-A" is superior (Which means that the specifications and characteristics of this turbine are more compatible with the study site), and the estimated values for mean power output, annual energy output, and CF after losses are 121 kW, 1,058,790 kWh, and 24.2% (Table 6), which shows a precise matching between turbine "WT-A" and the study area.

Table 6: Energy production and capacity factor of wind turbines throughout the year.

Hub height (m)	Wind Turbines	Mean Power Output (kW)		Annual Energy Output (kWh/yr)		NCF (%)	
		Before losses	After losses	Before losses	After losses	Before losses	After losses
50	WT-A	94.9	78.1	830,913	683,832	19.0	15.6
	WT-B	44.3	36.6	367,655	319,036	13.0	11.0
	WT-C	13.4	11.0	117.261	96.504	13.4	11.0
	WT-D	9.20	7.57	80,624	66,352	11.5	9.5
70	WT-A	119	98.2	1,044,780	859,842	23.9	19.6
	WT-B	56.7	46.6	496,315	408,462	17.2	14.1
	WT-C	16.9	13.9	147,905	121,725	16.9	13.9
	WT-D	11.8	9.72	103,454	85,141	14.8	12.1
100	WT-A	147	121	1,286,518	1,058,790	29.4	24.2
	WT-B	71.4	58.8	625,596	514,858	21.6	17.8
	WT-C	21.0	17.3	183,802	151,267	21.0	17.3
	WT-D	15.0	12.3	130,971	107,787	18.7	15.4

5.9 Net Power, Energy, and Capacity Factor

Figure 14 compares the four selected turbines in terms of net mean power output, net mean energy production, and net capacity factor at different heights. It is possible to know how the net power produced from the four chosen wind turbines changes during the hours of the day or the months of the year at 50 m, 70 m, and 100 m heights from Figures 14 (a and b), respectively. It is clear that the net mean power output increases during the daily hours after 6 AM, reaching its peak value at 7 PM; the output power rates increase during the summer months, reaching their highest value in June.

The comparison between the four selected turbines in terms of energy output is shown in Figures 14 (c and d). The net energy output from the four chosen wind turbines changes during the hours of the day or the months of the year at 50 m, 70 m, and 100 m heights. It is clear that the energy output increases during the daily hours after 6 A.M., reaching its peak value at 7 P.M. The net mean energy output increases during the summer months, reaching its highest value in June. The capacity factor behaves similarly to proceeding net mean power output and net mean energy output (daily or monthly) .

As depicted in Figure 14, it can be seen that the wind turbine WT-A is superior to other types of turbines and has a higher mean power output, annual energy production, and net capacity factor (Table 6). The higher capacity factor values 15.6, 19.6, and 24.2 at heights of 50 m, 70 m, and 100 m indicate the high matching between a wind turbine and the study area.

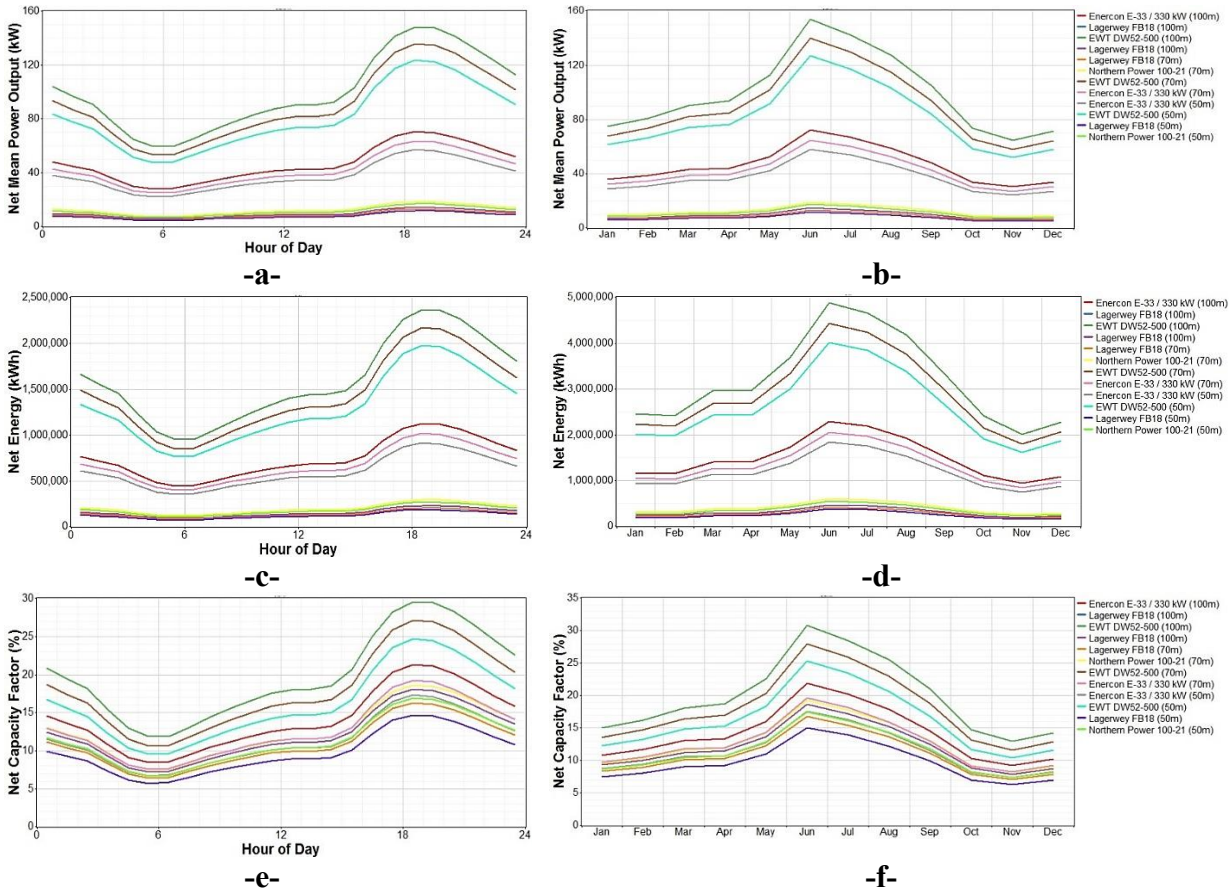

Figure 14: Comparison of the selected wind turbines' power, energy, and capacity factor production at different heights.

6. Conclusion

Wind energy quantitative measurement was accomplished in Sinjar to study the Wind Power Density through Weibull probability distributions from the attained wind speeds for 44 years. Data gathered from the NASA website and the wind characteristics and power potential of Sinjar were considered using wind measurements at 30 m, 70 m, and 100 m heights. From statistical analysis, it is evident that wind speed increases during the day 1 time period between 6 AM and 7 PM, which is suitable for daily time consumption. On the other hand, there is an increase in wind speed in the summer months, which may support electricity demand. Comparing the Weibull parameters performance, least squares performed better where R^2 demonstrated the best fit, which equals 0.996 at 50 m, 70 m, and 100 m heights, respectively. The wind rose diagram showed the direction of the West's dominant wind speed in the studied area. The overall mean wind speeds are found to be 4.657, 4.840, and 5.027 m/s at 50, 70, and 100 m, respectively, with corresponding mean Weibull shape parameter values k as 2.026 at three heights, while the corresponding mean Weibull scale parameter values *A* as 5.256, 5.463 and 5.649 m/s at 50, 70 and 100 m; respectively. Mean potential wind power and energy density values were found for a year of study as 116.7, 130.9, and 146.8 W/m^2 and 965, 1083, and 1814 kWh/m^2. Out of four turbines proposed for determining their productivity on site, turbine WT-A was the best. That is because the capacity factor values of this type are the highest at three heights; this is due to the high compatibility of the turbine with the study area, or in other words, the suitability of the turbine properties (v_c, v_r, and v_f) with the winds of the area. Therefore, this type of turbine with the exact specifications can be adopted to construct a wind farm in this region.

References

[1] M. Al-Ghriybah, "Assessment of wind energy potentiality at ajloun, jordan using weibull distribution function," 2022.

[2] N. Winter, "Renewables Global Status Report (GSR) Collection 2023-Transport Module Factsheet," 2023.

[3] O. S. A.-D. Al-Yozbaky and S. I. Khalel, "The future of renewable energy in Iraq: Potential and challenges," *Indonesian Journal of Electrical Engineering and Informatics (IJEEI),* vol. 10, no. 2, pp. 273-291, 2022.

[4] Z. S. Hussain, S. Alhayali, Z. E. Dallalbashi, T. Salih, and M. K. Yousif, "A look at the wind energy prospects in Iraq," in *2022 International Conference on Engineering & MIS (ICEMIS)*, 2022: IEEE, pp. 1-7.

[5] I. Citaristi, "International energy agency—iea," in *The Europa directory of international organizations 2022*: Routledge, 2022, pp. 701-702.

[6] F. A. Hadi, B. Abdulsada Al-Knani, and R. A. Abdulwahab, "An assessment the wind potential energy as a generator of electrical energy in the coastal area of southern Iraq," *Scientific Review Engineering and Environmental Sciences,* vol. 29, no. 1, pp. 37-53, 2020.

[7] A. S. Darwish, S. Shaaban, E. Marsillac, and N. M. Mahmood, "A methodology for improving wind energy production in low wind speed regions, with a case study application in Iraq," *Computers & Industrial Engineering,* vol. 127, pp. 89-102, 2019.

[8] S. V. Valentine, "Emerging symbiosis: Renewable energy and energy security," *Renewable and sustainable energy reviews,* vol. 15, no. 9, pp. 4572-4578, 2011.

[9] M. T. Chaichan and H. A. Kazem, *Generating electricity using photovoltaic solar plants in Iraq*. Springer, 2018.

[10] R. A. Abdulwahab, L. A. Al-Ani, and A. H. Shaban, "Fused images based on division of hyperspectral images into spectral groups," in *AIP Conference Proceedings*, 2023, vol. 3018, no. 1: AIP Publishing LLC, p. 020009.

[11] R. A. Abdulwahab, L. A. Al-Ani, and A. H. Shaban, "Hyperspectral pansharpening improvement using MNF transformation," in *AIP Conference Proceedings*, 2023, vol. 3018, no. 1: AIP Publishing LLC, p. 020052.

[12] A. A. Shestakova, "Impact of land surface roughness on downslope windstorm modelling in the Arctic," *Dynamics of Atmospheres and Oceans,* vol. 95, p. 101244, 2021.

[13] J. K. Lundquist, "Wind shear and wind veer effects on wind turbines," in *Handbook of Wind Energy Aerodynamics*: Springer, 2022, pp. 1-22.

[14] F. A. Hadi, S. S. Oudah, and R. A. Al-Baldawi, "Pre-feasibility study of hypothetical wind energy project using simulated and measured data," in *2018 2nd International Conference for Engineering, Technology and Sciences of Al-Kitab (ICETS)*, 2018: IEEE, pp. 60-65.

[15] B. Yan, Q. Li, P. Chan, Y. He, and Z. Shu, "Characterising wind shear exponents in the offshore area using Lidar measurements," *Applied Ocean Research,* vol. 127, p. 103293, 2022.

[16] P. K. Sharma, V. Warudkar, and S. Ahmed, "Effect of atmospheric stability on the wind resource extrapolating models for large capacity wind turbines: A comparative analysis of power law, log law, Deaves and Harris model," *Energy Procedia,* vol. 158, pp. 1235-1240, 2019.

[17] E. Nymphas and R. Teliat, "Evaluation of the performance of five distribution functions for estimating Weibull parameters for wind energy potential in Nigeria," *Scientific African,* vol. 23, p. e02037, 2024.

[18] S. Mathew, *Wind energy: fundamentals, resource analysis and economics*. Springer, 2006.

[19] I. K. Rotich and P. K. Musyimi, "Wind power density characterization in arid and semi-arid Taita-Taveta and Garissa counties of Kenya," *Cleaner Engineering and Technology,* vol. 17, p. 100704, 2023.

[20] K. A. MAHMOUD, S. A. IBRAHIM, I. N. MOHSIN, and Z. M. KLARI, "IDENTIFYING THE BEST-FIT PROBABILITY DISTRIBUTION MODEL TO PREDICT THE ANNUAL MAXIMUM DAILY RAINFALL IN DUHOK CITY, IRAQ," *Journal of Duhok University,* vol. 26, no. 2, pp. 13-23, 2023.

[21] Z. H. Hulio, W. Jiang, and S. Rehman, "Techno-Economic assessment of wind power potential of Hawke's Bay using Weibull parameter: A review," *Energy Strategy Reviews,* vol. 26, p. 100375, 2019.

[22] G. H. Shakir and I. Hassan, "Study of new Exponential-Weibull distribution about children with Leukemia," in *AIP Conference Proceedings*, 2024, vol. 3036, no. 1: AIP Publishing LLC, p. 040030.

[23] G. Silva, A. Pereira, D. Faro, and E. Feitosa, "On the accuracy of the Weibull parameters estimators," in *European Wind Energy Conference and Exhibition (EWEC). London UK*, 2004.

[24] F. A. Hadi, "Optimum Selection of Wind Turbines Using Normalized Power and Capacity Factor Curves," *Iraqi Journal of Science,* 2021.

[25] S. Carreno-Madinabeitia, G. Ibarra-Berastegi, J. Sáenz, and A. Ulazia, "Long-term changes in offshore wind power density and wind turbine capacity factor in the Iberian Peninsula (1900–2010)," *Energy,* vol. 226, p. 120364, 2021.

[26] A. Nurlatifah, A. Pratama, and P. Maria, "Indonesia offshore wind energy: Initial wind resource potential perspective from dataset reanalysis," in *AIP Conference Proceedings*, 2021, vol. 2366, no. 1: AIP Publishing.